This document was prepared in conjunction with work accomplished under Contract No. DE-AC09-96SR18500 with the U. S. Department of Energy.

DISCLAIMER

WSRC-TR-2005-00470

Scoping Calculations of Tank 48 Vapor Space Mixing

Si Young Lee
Richard A. Dimenna

October 2005

Westinghouse Savannah River Company
Savannah River National Laboratory
Aiken, SC 29808

Prepared for the U.S. Department of Energy
Under Contract No. DE-AC09-96SR18500

SRNL
SAVANNAH RIVER NATIONAL LABORATORY

DISCLAIMER

Printed in the United States of America

Prepared For

U.S. Department of Energy

WSRC-TR-2005-00470

Keywords: Computational Fluid Dynamics, Tank 48 Vapor Space, Flow Patterns, Benzene Concentration

Scoping Calculations of Tank 48 Vapor Space Mixing

Si Young Lee

Richard A. Dimenna

October 2005

Westinghouse Savannah River Company
Savannah River National Laboratory
Aiken, SC 29808

Prepared for the U.S. Department of Energy

Under Contract No. DE-AC09-96SR18500

SRNL
SAVANNAH RIVER NATIONAL LABORATORY

Review and Approvals

S. Y. Lee, Author — Date 10/12/05
Eng. Modeling and Simulation Group, SRNL

R. A. Dimenna, Coauthor — Date 10/12/05
Eng. Modeling and Simulation Group, SRNL

G. A. Taylor, Technical Reviewer — Date 10/13/05
Waste Processing Tech. Section, SRNL

S. C. Shah, Customer Reviewer — Date 10/13/05
Tank 48 Disposition Project / LWDP

C. P. Holding-Smith, Manager — Date 10/13/05
Eng. Modeling and Simulation Group, SRNL

D. T. Conrad, DA Manager — Date 10/13/05
Tank 48 Disposition Project / LWDP

R. H. Spires, Project Owner — Date 10-13-05
Tank 48 Disposition Project / LWDP

Table of Contents

List of Figures

List of Tables

Abstract

Scoping calculations to address the mixing behavior of benzene in the vapor space of Tank 48 and estimate maximum benzene concentrations have been completed. The analysis was focused on determining whether a detailed assessment using a computational fluid dynamics (CFD) model of the Tank 48 vapor space could support Safety Class calculations. The calculations included nominal boundary conditions for air inlet and exhaust flows, as well as benzene evolution from the tank liquid surface. Additional calculations included a reduced benzene evolution rate, reduced air inlet and exhaust flows, and a modified air inlet location. The calculations were based on prototypic tank geometry and nominal operating conditions as defined by the Closure Business Unit.

The results showed that the vapor space was fairly well mixed and that benzene concentrations were relatively low for typical operating conditions. All the calculations addressing sensitivity issues such as differencing options, mesh density, and transient performance in the model demonstrated that the scoping model could capture the necessary phenomena without introducing nonphysical behavior because of the numerical discretization. Therefore, refining and upgrading the present scoping model is feasible for support of safety class calculations.

1. Introduction

Closure Business Unit Engineering has been evaluating flammability conditions in the vapor space of Tank 48 in association with the safety analysis. In order to help assess the benzene concentration in the vapor space, Savannah River National Laboratory (SRNL) was requested to develop a computational model to estimate the degree of benzene mixing for nominal conditions of purging airflow and benzene since airflow behavior is similar to the actual purging gas of nitrogen. The geometrical configurations for the tank vapor space are shown in Fig. 1.

The objective of the work is to perform scoping calculations for the benzene mixing behavior in the vapor space of Tank 48 and its impact on the local concentration of benzene. The calculations will be used to evaluate the degree to which purge air mixes with benzene evolving from the liquid surface and its ability to prevent an unacceptable concentration of benzene from forming. The principal air flow ventilation path is included with a model representing the major features of the Tank 48 vapor space. The results will be used to decide whether to refine the calculations and upgrade the scoping model to allow the analysis to be used for safety significant guidance.

A computational fluid dynamics (CFD) model was developed to evaluate air flow patterns and estimate benzene concentration in the vapor space. The modeling domain represents the major features of the Tank 48 and includes the principal air flow ventilation path of the Tank 48 vapor space including the central concrete support column as shown in Fig. 1.

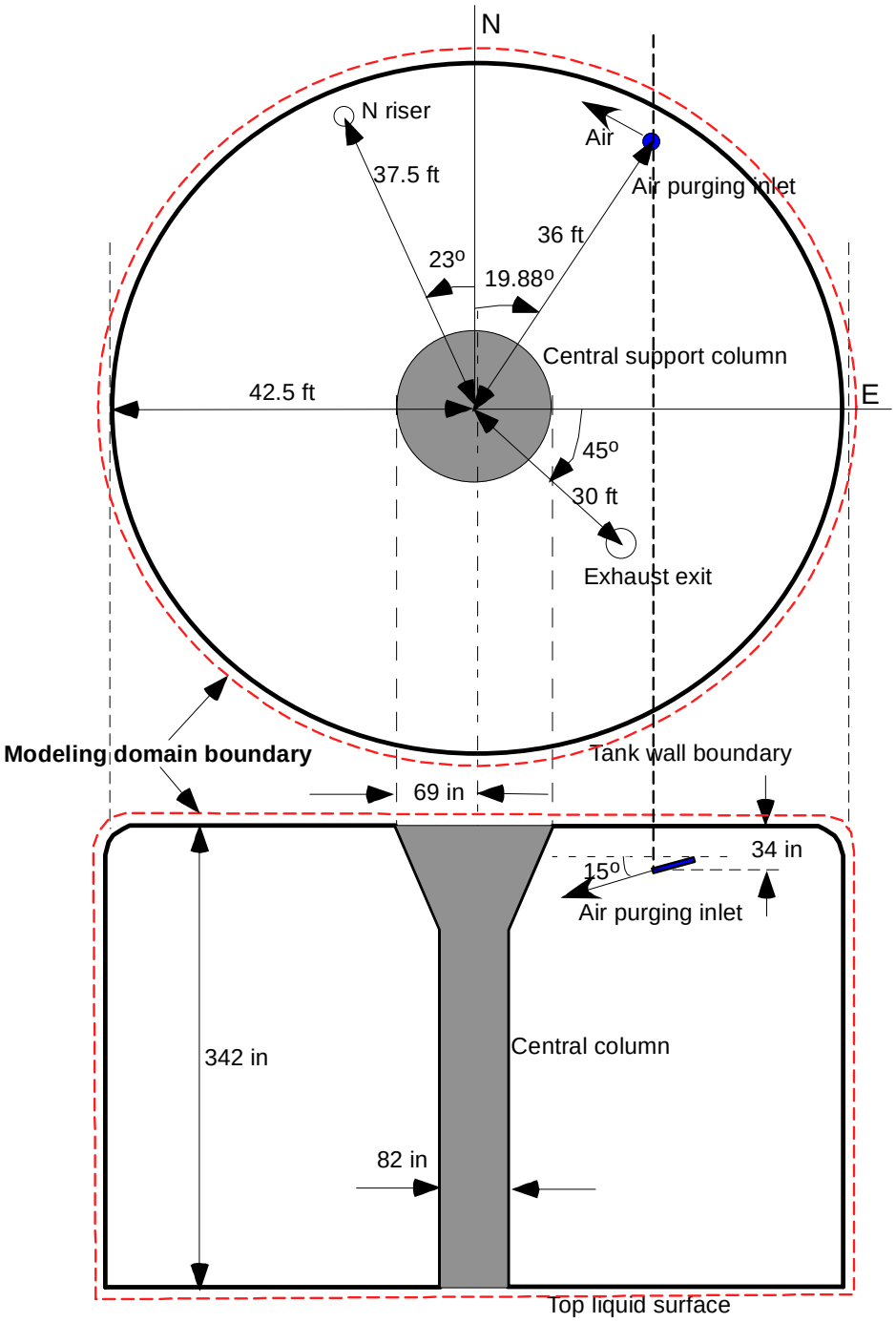

Figure 1. Modeling domain boundary used for the present scoping calculations

2. Modeling Approach and Analysis Method

A three-dimensional approach was taken to model the gas space of Tank 48. A finite volume CFD code, FLUENT™ [4], was used to perform the analysis. A standard two-equation, k-ε model, was used to estimate the gas turbulence. Thus, the governing equations to be solved are composed of one mass balance, three momentum equations for the three-dimensional space, two turbulence equations, and one benzene transport equation for benzene gas. The computational domain boundary used for the present calculations is shown in Fig. 1.

Modeling assumptions for the scoping calculations are as follows:

- Single exhaust location from the vapor space
- Single gas injection location for a given calculation. The injection point may be changed as a sensitivity parameter [2].
- Benzene evolution rate from the liquid space is constant and uniform.
- Cooling coils in the vapor space have no impact on gas flow patterns.
- Air leakage into the vapor space is negligible.
- Temperature is constant, so thermally driven convection can be ignored.
- No chemical reactions during the benzene transport and mixing process.
- Benzene gas is a dilute mixture component, so the mass diffusion coefficient is independent of gas composition.
- Acceptance criteria for local benzene concentration will be provided by the customer organization. For the scoping calculations, 25% of local benzene LFL, 1.37 benzene vol.%, is used as an acceptance criterion.

Based on the three-dimensional computation domain of Fig. 1 and the modeling assumptions, benzene mass fractions for the modeling cases are computed under steady-state or transient operating conditions. The cases considered here and the material properties used for the calculations are shown in Table 1 and Table 2. All of the basic cases used a second order differencing scheme in order to minimize the numerical diffusion caused by the discretization.

The flow conditions for the vapor space during the air purging operation are assumed to be fully turbulent since Reynolds numbers for typical 300 scfm operation are in the range of 500,000 based on the inlet conditions of the 1-in nozzle. A standard two-equation turbulence model, the k–ε model [4], was used since previous work [5] showed that the two-equation model predicts the flow evolution of turbulent flow in a large stagnant fluid domain with reasonable accuracy. The model is a full three-dimensional representation of the entire gas space to capture significant circulation phenomena related to the turbulent behavior of the gas flow.

Air was used to simulate the gas in the vapor space. Although nitrogen is used as a purging gas instead of air, its flow pattern and mixing behavior are expected to be similar to those of air under the same operating conditions. Governing equations for the entire computational domain were solved with FLUENT™ [4] for different cases in steady-state and transient simulation modes. They are the initial reference and the sensitivity cases as shown in Table 1. The major material and physical properties used for the calculations are listed in Table 2.

Table 1. Modeling conditions used for the sensitivity runs [1, 2]

Cases	**Purpose**		**Air inlet location and size**	**Air flowrate at inlet (ft^3/min)**	**Benzene generation (gm/min)**
Reference	Initial test case		C3(1-in dia.)	300	400
Case-1	Nominal mesh		C3(1-in dia.)	300	50
Case-1A	Numerical sensitivity	Finer mesh	C3(1-in dia.)	300	50
Case-1B		Numerical differencing	C3(1-in dia.)	300	50
Case-1C		Dynamic response	C3(1-in dia.)	300	50
Case-2	Physical sensitivity		C3(1-in dia.)	150	50
Case-3	Physical sensitivity		N(6-in dia.)	150	50

Table 2. Material properties and modeling conditions

Parameters	Input data
Air density	1.225 kg/m^3
Benzene vapor density	3.3 kg/m^3
Benzene molecular diffusion coefficient in air	8.8 x 10^{-5} m^2/sec [3]
Turbulent Schmidt number*	0.7

Note:*: Ratio of turbulent viscosity to mass diffusion

3. Results and Discussions

The present model for the scoping calculations employed a three-dimensional CFD approach with two-equation turbulence model described in terms of turbulent dissipation and eddy diffusivity, referred to as k-ε model in the literature.[6] It assumed isothermal conditions for the gas medium so that natural convection was not included. The computational domain is shown in Fig. 2.

The primary objective of the work was to estimate maximum benzene concentration under the potential operating conditions. The model actually computes benzene mass fractions. The benzene volume fraction is obtained from the computed mass fraction using a gas density ratio of benzene vapor to air of about 2.7. Graphical results are presented in Fig. 3. Table 3 also shows numerical values of the benzene volume concentrations corresponding to benzene mass fractions. The benzene LFL concentration of 1.37 vol.% corresponds to a mass fraction of 0.036.

The analysis considered four different cases of operating conditions. Before completing those runs, a series of test runs was conducted to evaluate the calculated sensitivity to the number of meshes, numerical differencing and transient system response to a sudden cessation of air flow at the inlet in order to establish the reliability of the solution method. All the cases are summarized in Table 1.

The model used two different meshes for the meshing sensitivity run, but the one-million mesh model was used for the initial test run. The computational meshes on a two-dimensional plane are presented in Fig. 4. The initial test case used 300 scfm airflow through a 1-in inlet nozzle in the C3 riser and 400 gm/min benzene evolution from the liquid region. This is the reference case of Table 1. The inlet velocity from 300 scfm airflow through a 1-in nozzle is about 280 m/sec. Figure 5 shows velocity distributions and benzene mass fraction contours at the vertical plane crossing the central line A-A' under the referenced initial conditions. The results show a maximum benzene mass fraction of about 0.043, corresponding to about 1.63 vol.%. It is noted that when benzene is perfectly mixed with air inside the tank gas space under the steady-state operating conditions for the reference case, benzene volume percent is about 1.41.

As shown in Figs. 6 and 7, the gas contained in the vapor space rotates counterclockwise around the central support column. This is consistent with the ventilation air inlet is located near the wall boundary and the air flow injected into the vapor space azimuthally with a 15^{o} downward orientation toward the tank bottom. Detailed flow patterns and velocity distributions for the vertical plane crossing the air inlet nozzle are shown in Fig. 8. The calculation shows that gas movement near the wall boundary region is much stronger than the region near the central column. As shown in Fig. 9, the central region has higher benzene concentrations compared to the wall boundary region. It is also noted that the benzene concentration gradient over the entire region of the vapor space is very small. The level of benzene concentration is about 20% higher than the LFL value of 1.37 benzene vol%. The calculation results show that the reference case does not support an acceptance criterion of 25% LFL, or 0.34 benzene vol.%.

When the benzene evolution rate is reduced from 400 gm/min to the Case-1 value of 50 gm/min, the maximum benzene concentration shows a commensurate reduction of about 88%. Figure 10 compares the results of the benzene concentrations between the two cases in terms of the benzene mass fraction. The diagrams in Figure 10 are each scaled to their own maxima as can be seen by the color scale on the left. Therefore, the diagrams can be compared to show that the nondimensional benzene distribution is similar for both cases. This result is to be expected because the driving flow, the air inlet, is the same in both calculations. When maximum values for both diagrams are set to the same color, red, as in Fig. 11, the entire plane for the Case-1 conditions is non-red. This means the benzene concentration in Case-1 is lower than the benzene LFL of 1.37 vol% everywhere, while the reference case is above the LFL concentration everywhere as indicated by the entire tank being red. Figures 10 and 11 both display the same calculations – only the color scales on the figures is different.

Figure 12 presents a comparison of velocity and benzene mass fraction distributions near the liquid surface inside Tank 48 for Case-1 conditions. Benzene concentrations at various horizontal planes above the liquid surface are shown using the same color scale in Fig. 13. It is noted that benzene concentration gradients over the entire region of the vapor space are consistently small because of the gas turbulence.

A series of sensitivity analyses was performed to evaluate the impact of the number of computational meshes, numerical differencing scheme, and dynamic system response on the numerical discretization error, referred to as numerical diffusion in the literature. About one million meshes were used for the nominal base cases such as Case-1, and about two million meshes were used for Case-1A with the finer mesh sizes to perform the sensitivity analysis. The calculations had identical operating conditions as shown in Table 1. The maximum mesh sizes for the two cases, Case-1 and Case-1A, were 9.6 and 6.5 inches, respectively. Figure 14 shows that the differences in velocity distributions between the coarser meshes of Case-1 and the finer meshes of Case-1A are negligibly small. Benzene concentration distributions at the central vertical and horizontal planes of the vapor space are compared in Figs. 15 and 16. The results demonstrated that the differences due to different mesh sizes are also negligibly small for the benzene concentration gradients. Based on these results, all the base cases used one million meshes.

Sensitivity results for different numerical differencing schemes were performed by using two different numerical approaches. The first case used the first-order numerical differencing scheme for the initial run, and then switched to a second-order scheme by restarting the problem from the final converged solution. The other approach used the second-order numerical scheme during the entire solution process. The calculations showed that no major difference resulted from using different differencing schemes.

Qualitative dynamic behavior was examined by stopping the air inlet flow at the initial transient time beginning from the steady-state operating conditions of Case-1. This case corresponds to Case-1C as shown in Table 1. Dynamic responses of Case-1C are compared with the Case-1 results at 3 minutes transient time in terms of benzene concentrations in the tank vapor space as shown in Fig. 17. The results show that the transient responses are qualitatively correct, i.e., the flow slows down and appears to be stopping in the absence of a driving force. All the sensitivity calculations demonstrate that the current number of meshes and solution method used for the scoping analysis provide reasonable numerical results.

When the inlet air flow is reduced from 300 scfm to 150 scfm as shown in Table 1, the inlet velocity magnitude is changed from about 280 m/sec to 140 m/sec. For a benzene generation rate of 50 gm/min corresponding to Case-2, the maximum benzene concentration increases from 0.20 vol% to 0.41 vol%. The results for Case-2 are compared with those of Case-1 in terms of velocity and benzene concentration distributions in Figs. 18 through 20. All the results show that benzene gas is well mixed by the purging air flow.

Lastly, when the inlet airflow of 150 scfm enters through the 6-in N riser instead of the 1-in nozzle in the C3 riser (Case-3), benzene concentration gradients are significantly different. The results show that maximum benzene concentration reaches about 0.46 vol%, compared to 0.41 vol% of Case-2. It is also noted that the average benzene concentration difference between the maximum and minimum values for Case-3 is about 150% of that seen in Case-2. Figure 21 compares the results between Case-2 and Case-3 using the same color scale. The results show that Case-3 has a more stratified benzene distribution than Case-2 because of less gas movement. Figure 22 shows benzene mass fractions for Case-3 scaled to the maximum value for this calculation. It shows that the benzene concentration ranges from 0.46 to 0.36 vol%. All the results for the cases considered here are summarized in Table 4.

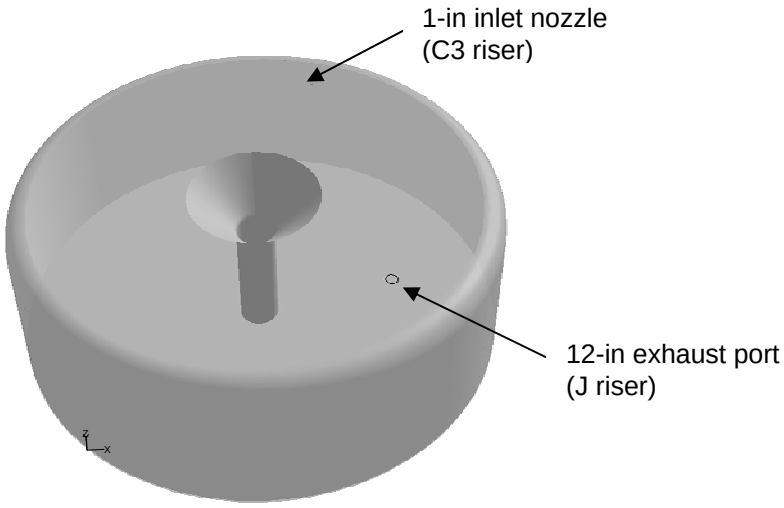

(Three-dimensional top view)

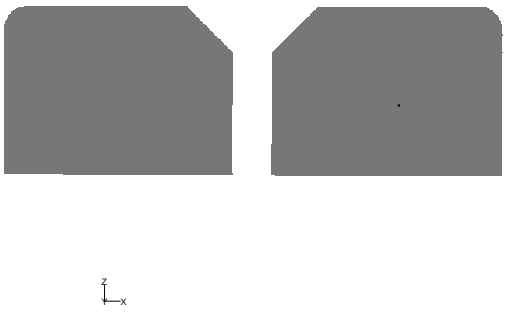

(Two-dimensional side view)

Figure 2. Computational domain as modeled for the calculations of benzene concentrations in the vapor space of Tank 48

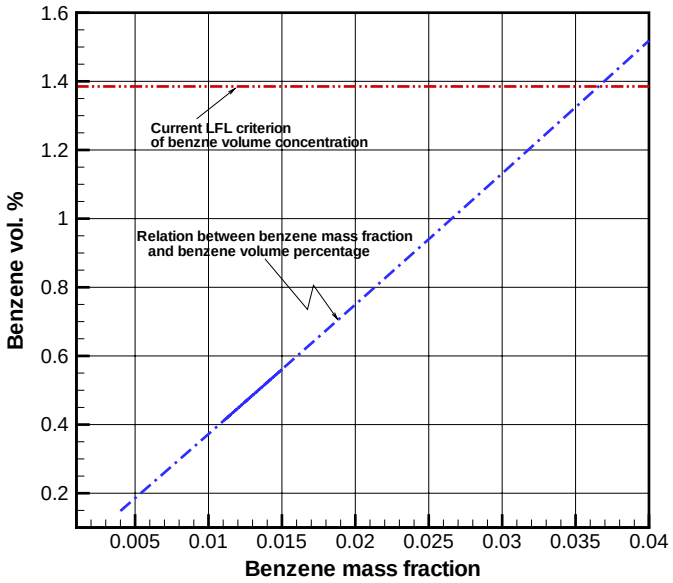

Figure 3. Benzene volume percentages for various benzene mass fractions

Table 3. Benzene volume percentages for various benzene mass fractions

C_6H_6 mass fraction	C_6H_6 vol.%	%LFL	C_6H_6 mass fraction	C_6H_6 vol.%	%LFL
0.0040	0.148	10.8	0.0150	0.560	40.9
0.0045	0.167	12.2	0.0200	0.750	54.7
0.0050	0.186	13.6	0.0250	0.940	68.6
0.0051	0.189	13.8	0.0300	1.132	82.6
0.0053	0.197	14.4	0.0350	1.325	96.7
0.0075	0.279	20.4	0.0362	1.370(LFL)	100
0.0100	0.372	27.2	0.0370	1.402	102
0.0104	0.386	28.2	0.0400	1.519	111
0.0110	0.410	29.9	0.0410	1.556	114
0.0123	0.459	33.5	0.0430	1.636	119

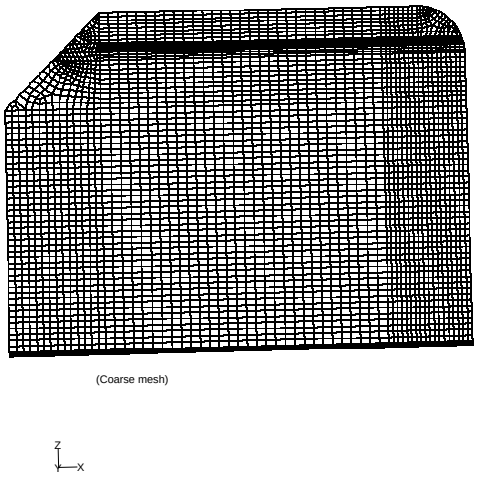

(Coarser meshes: about 1 million meshes)

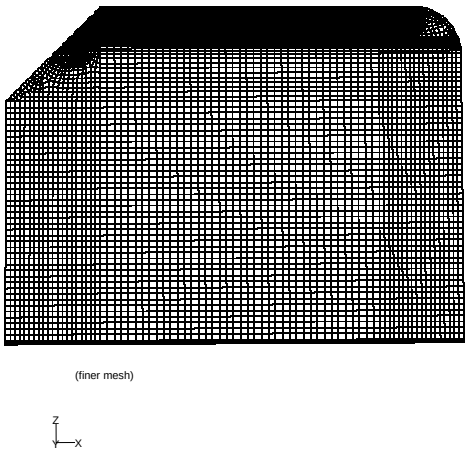

(Finer meshes: about 2 million meshes)

Figure 4. Coarser and finer meshes as used for the mesh sensitivity runs

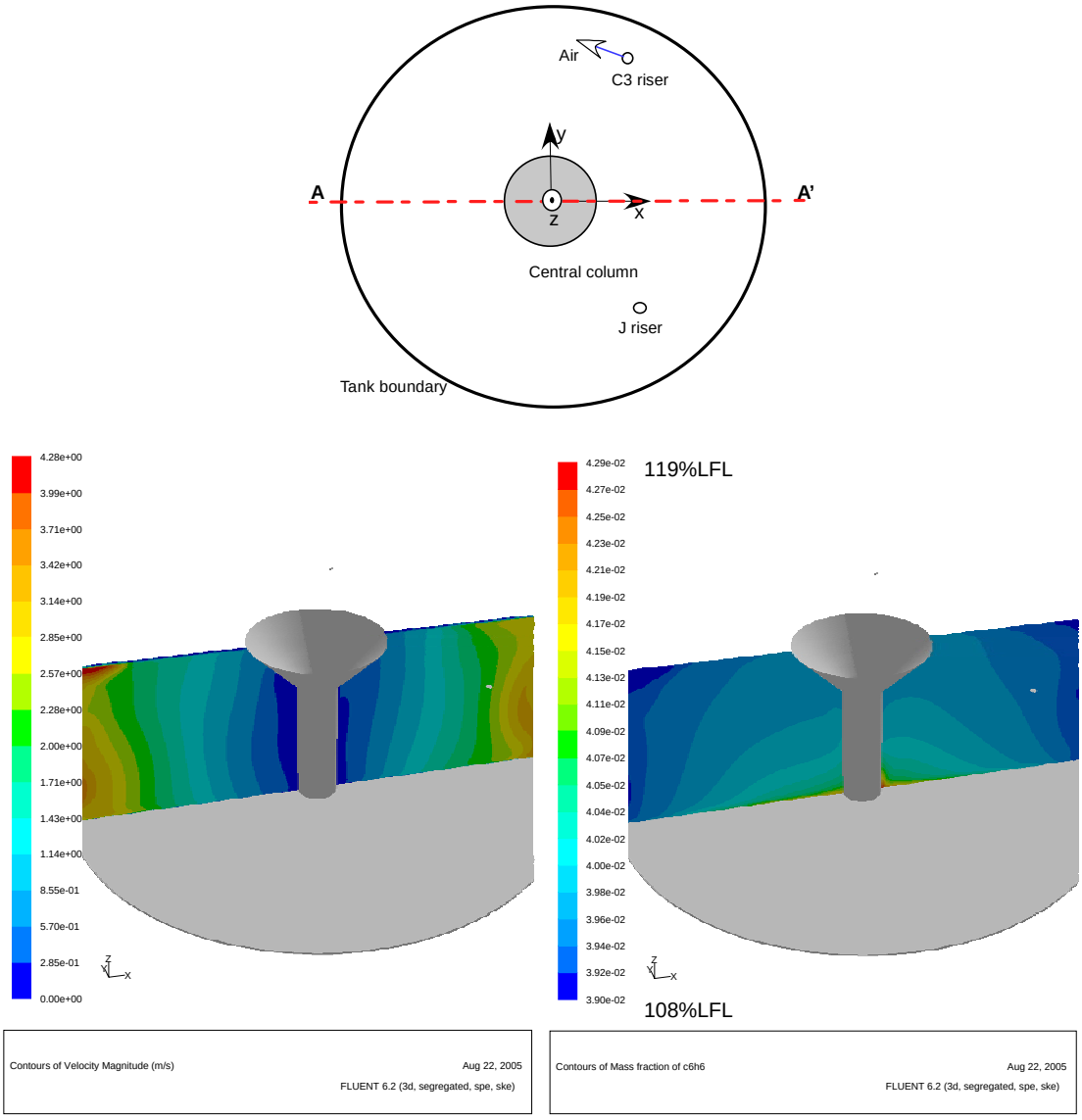

(Velocity distributions) (Benzene mass fraction contour)

Figure 5. Velocity distributions and benzene mass fraction contours at the vertical plane crossing the central line A-A' under the referenced initial conditions

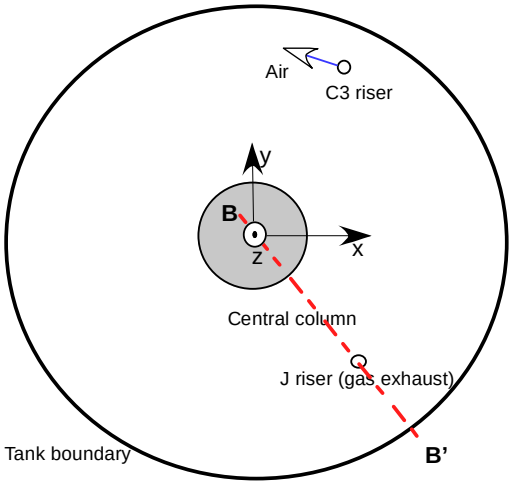

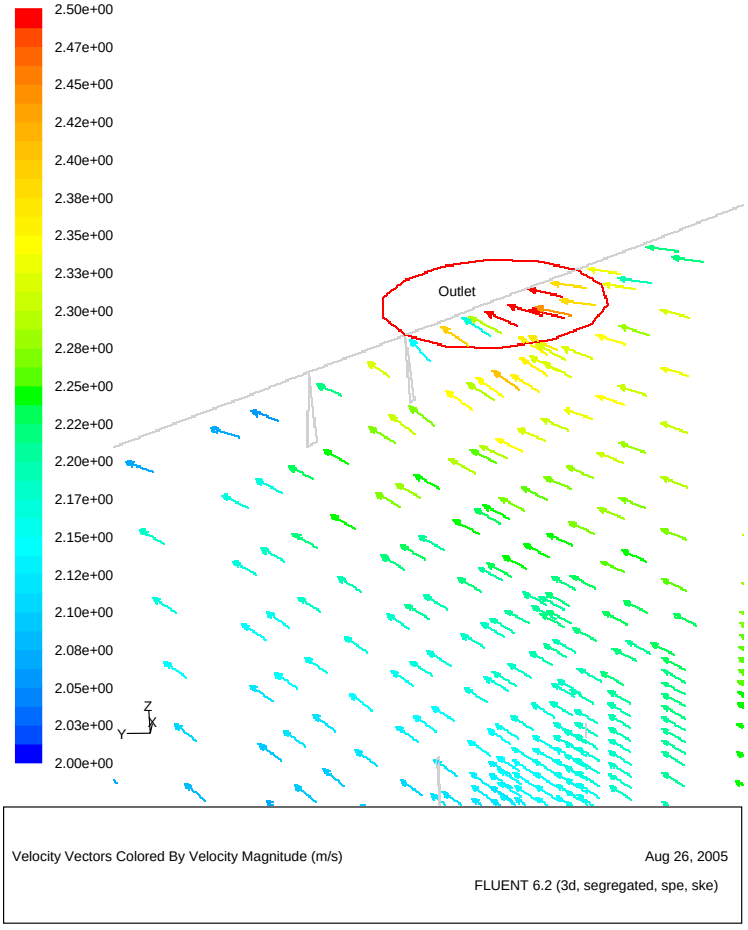

Figure 6. Flow patterns near the gas exhaust area at the vertical exit plane crossing the central line B-B' for the initial reference case (400 gm/min benzene generation rate and 300 cfm airflow through C3 riser)

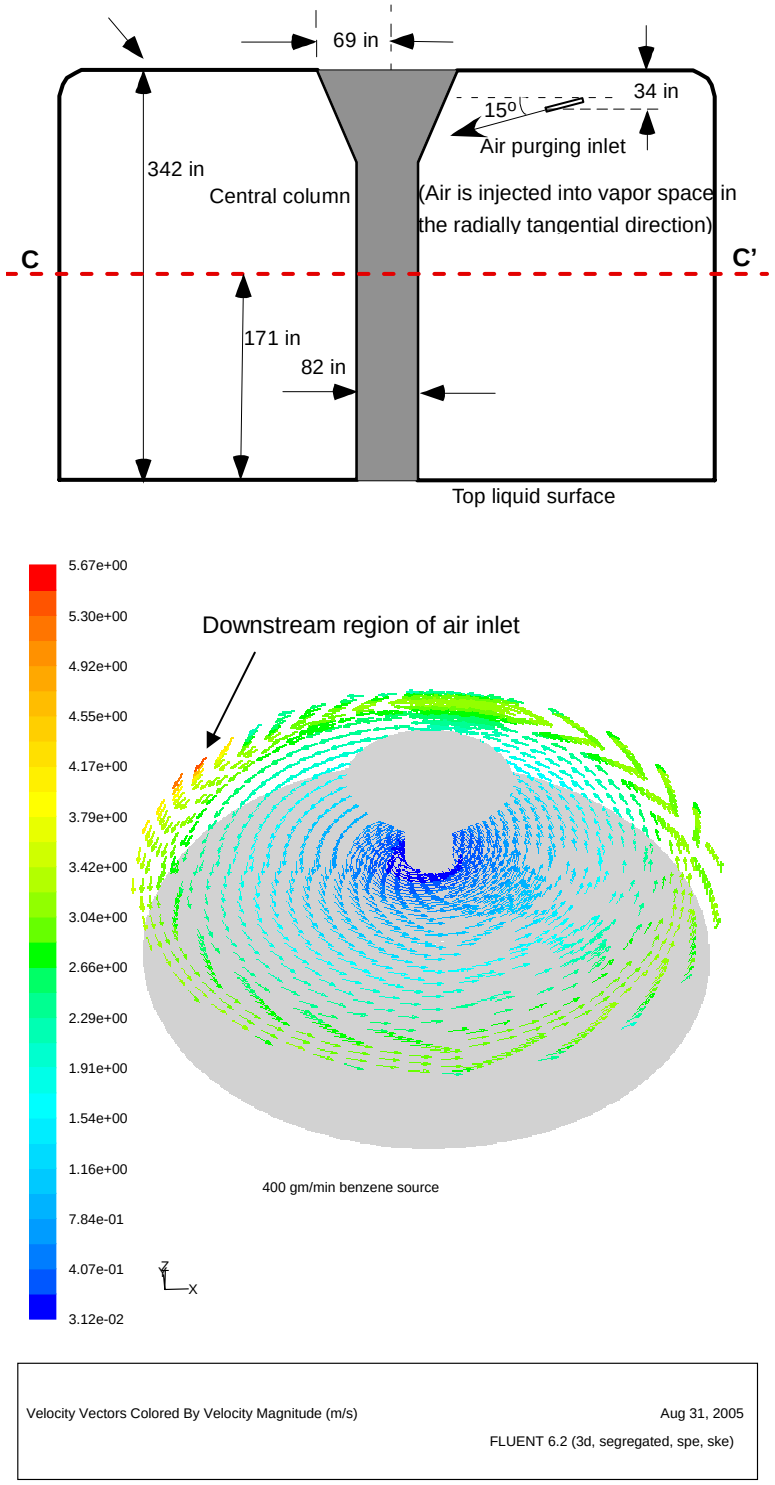

Figure 7. Flow patterns at the mid-plane for 400 gm/min benzene generation rate and 300 cfm airflow through C3 riser at the horizontal plane of Tank 48 crossing the line C-C'

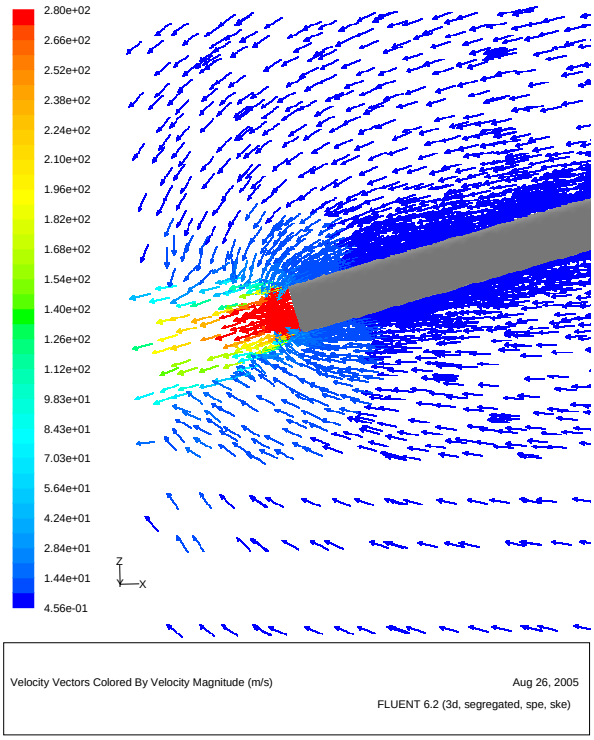

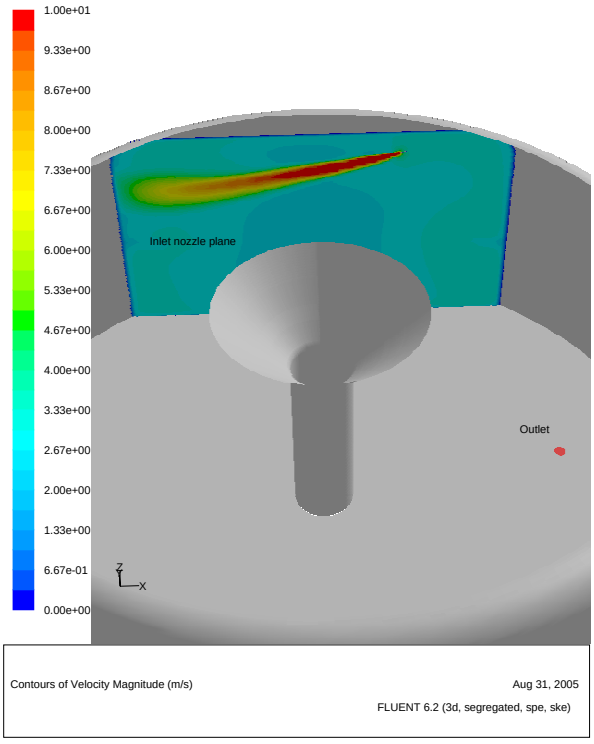

Figure 8. Flow patterns and contours for 400 gm/min benzene generation rate and 300 cfm airflow through C3 riser at the nozzle plane of Tank 48

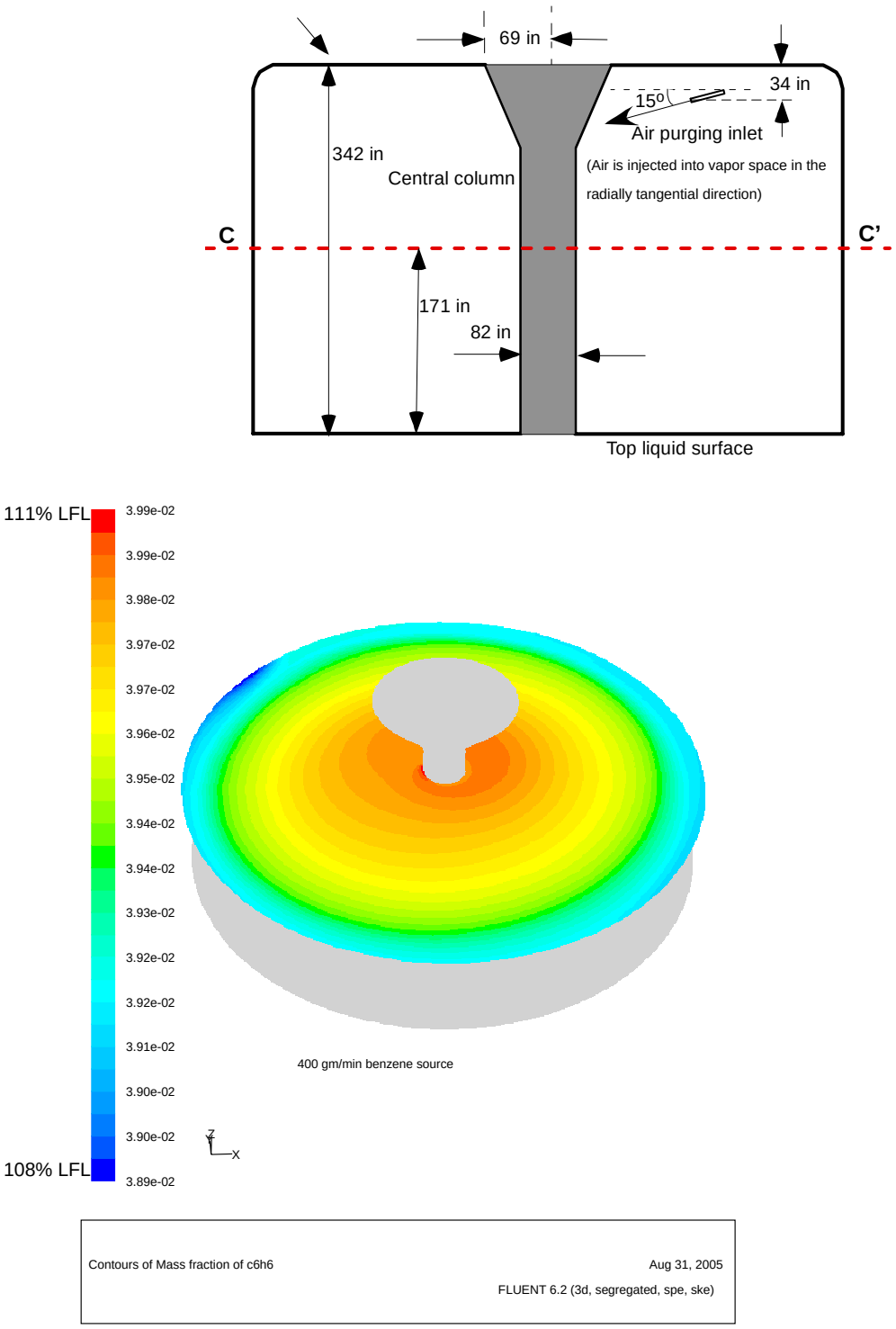

Figure 9. Benzene mass fraction distributions at the mid-plane for 400 gm/min benzene generation rate and 300 cfm airflow through C3 riser at the horizontal plane crossing the mid-height line C-C' of the vapor space

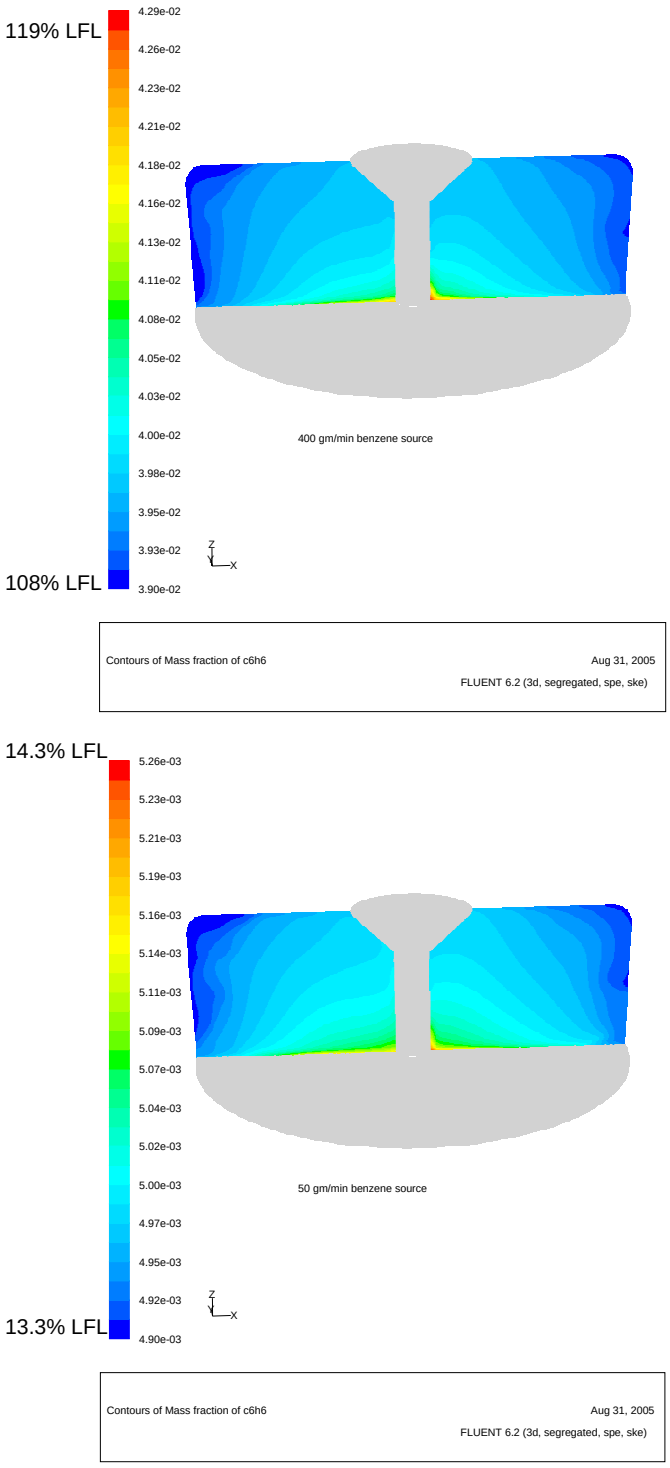

Figure 10. Comparison of benzene mass fraction distributions between 400 gm/min and 50 gm/min benzene generation rate under 300 cfm airflow through C3 riser at the central plane of Tank 48 (0.0362 mass fraction corresponds to 1.37 C6H6 vol%)

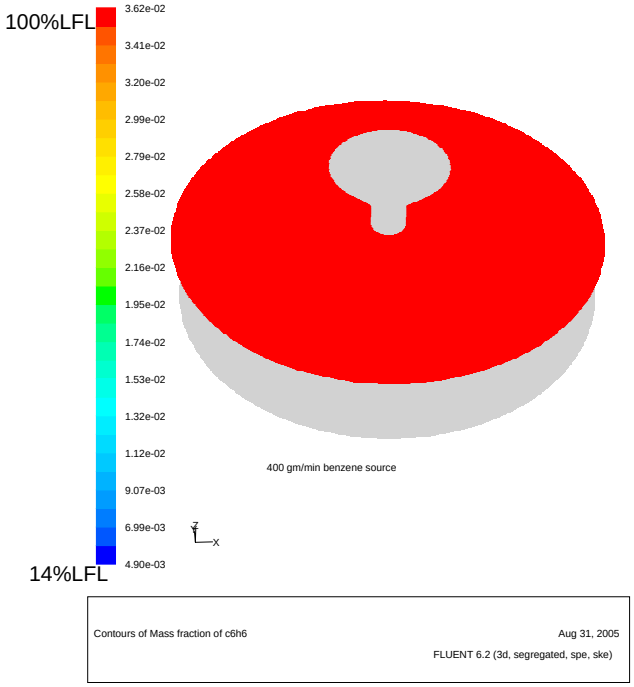

(Reference)

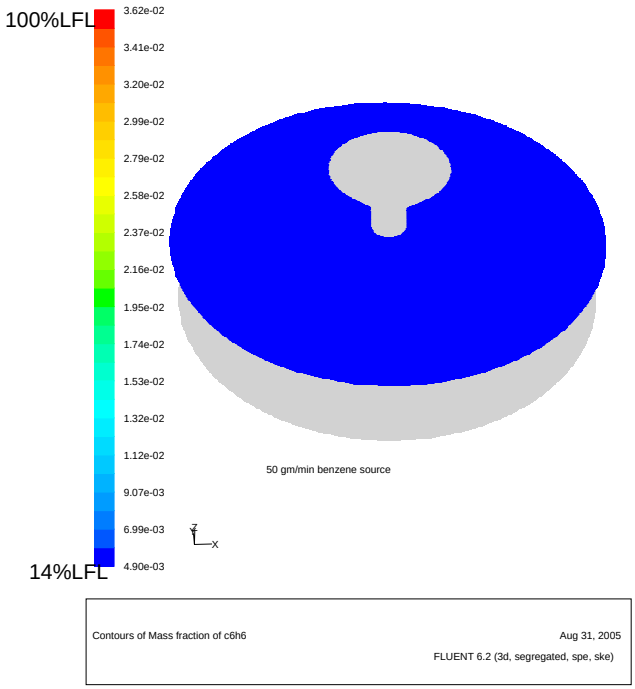

(Case-1)

Figure 11. Comparison of benzene mass fraction distributions between 400 gm/min and 50 gm/min benzene generation rate under 300 cfm airflow through C3 riser at the central plane of Tank 48 (0.0362 mass fraction corresponds to 1.37 C6H6 vol%)

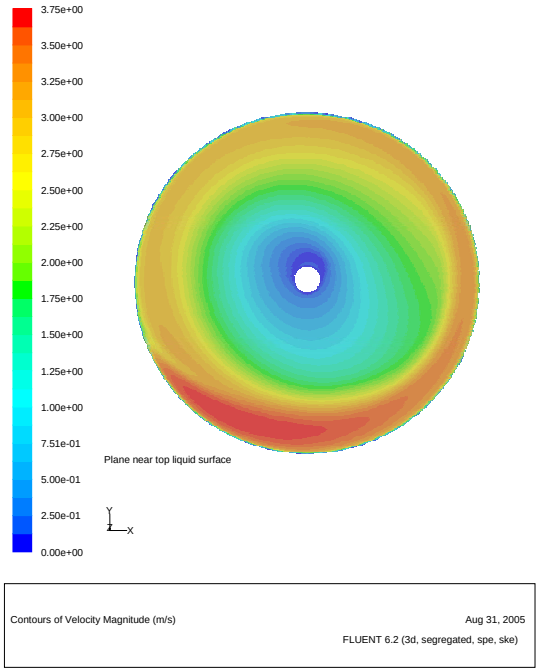

(Velocity contour)

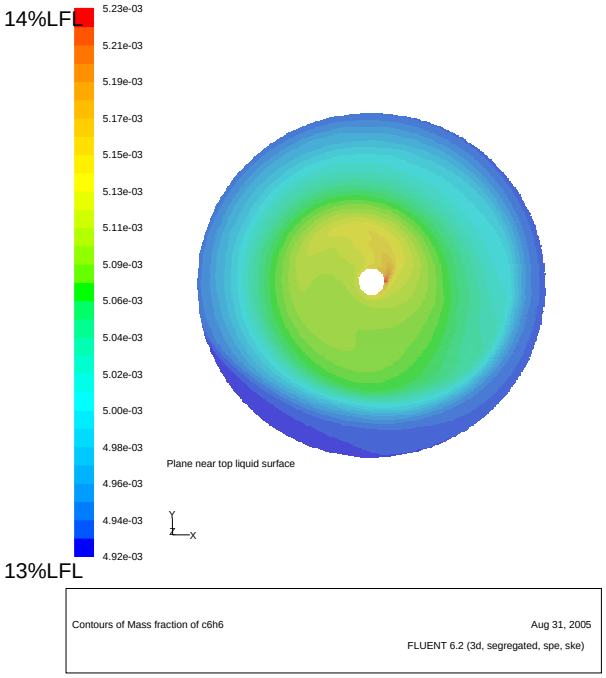

(Benzene mass fraction contour)

Figure 12. Comparison of velocity and benzene mass fraction distributions near the surface of liquid region inside Tank 48 under 300 scfm air purging flow through the nozzle of C3 riser and 50 gm/min. benzene generation rate (Case-1)

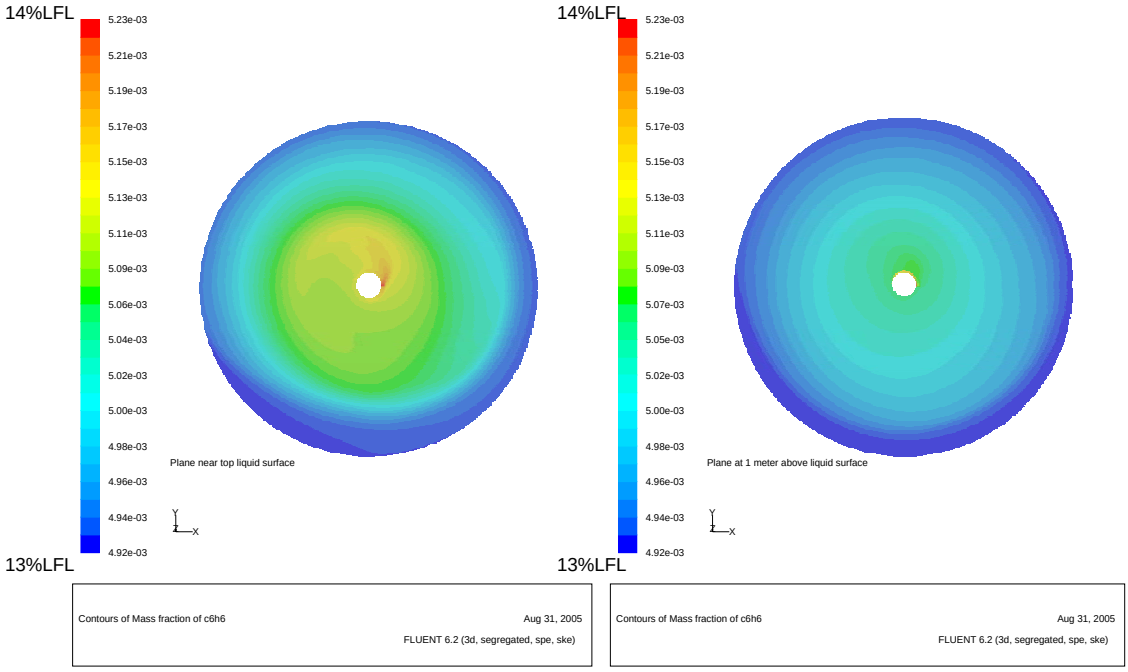

(Near the liquid surface) (About 40 in above the liquid surface)

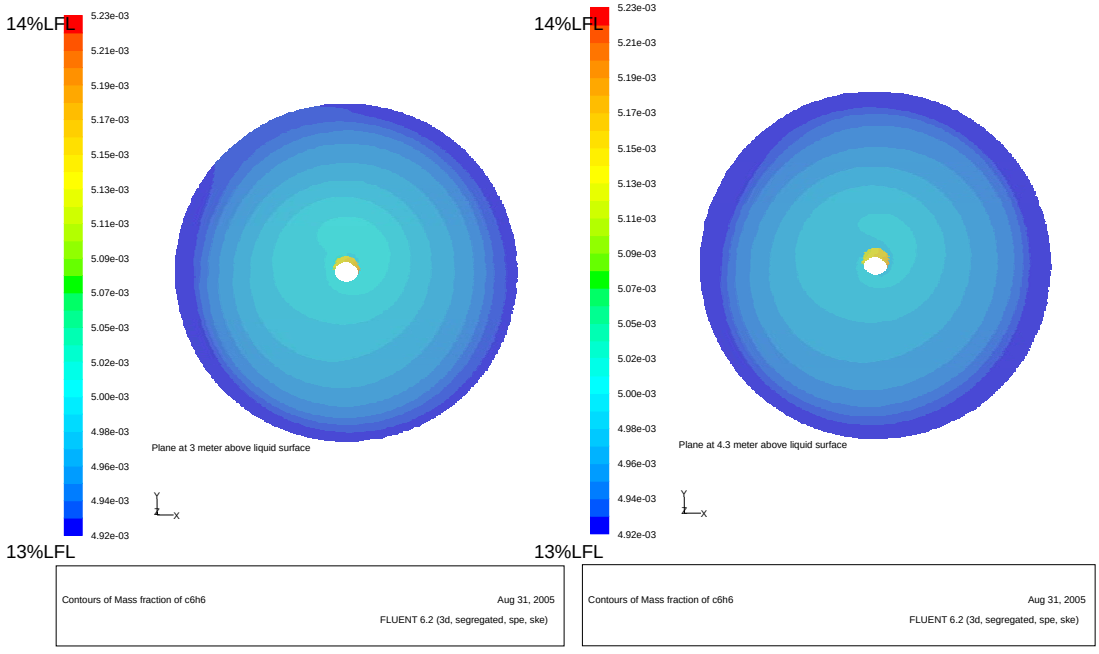

(120 in above the liquid surface) (171 in above the liquid surface)

Figure 13. Benzene mass fractions under the same scaling system for various elevations from the top surface of liquid region indicating that benzene concentration gradients for the vapor space are very small. (Case-1)

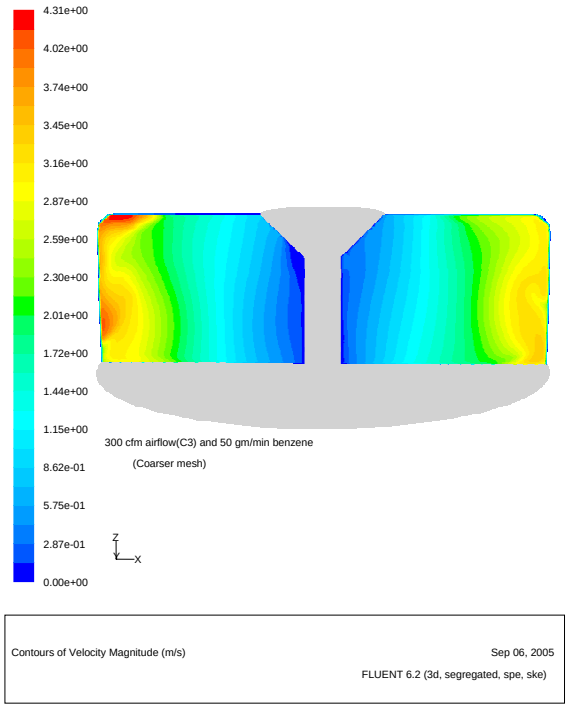

(Case-1: 300 cfm airflow and 50 gm/min benzene generation rate with about 1 million nodes)

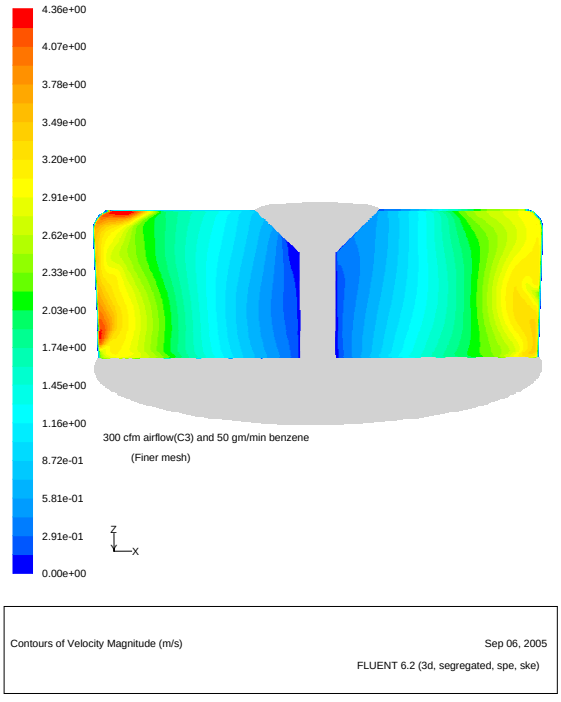

(Case-1A: 300 cfm airflow and 50 gm/min benzene generation rate with about 2 million nodes)

Figure 14. Comparison of gas flow contours between the two cases

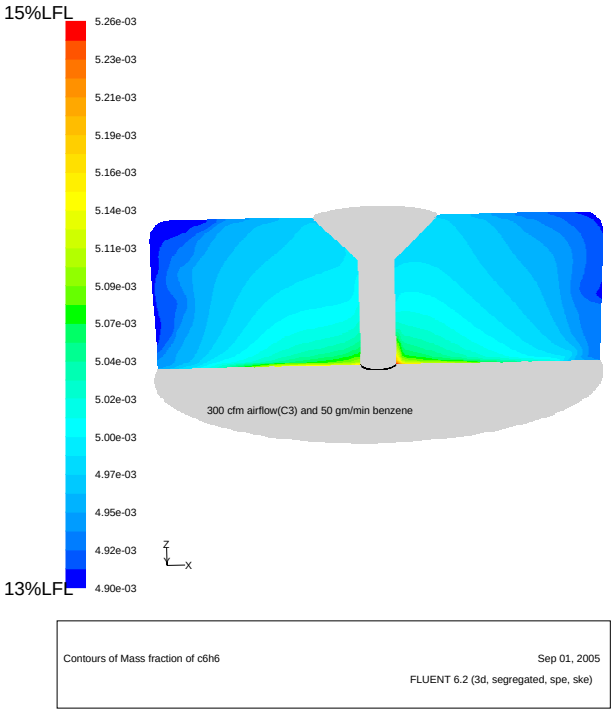

(Case-1: 300 cfm airflow and 50 gm/min benzene generation rate with about 1 million nodes)

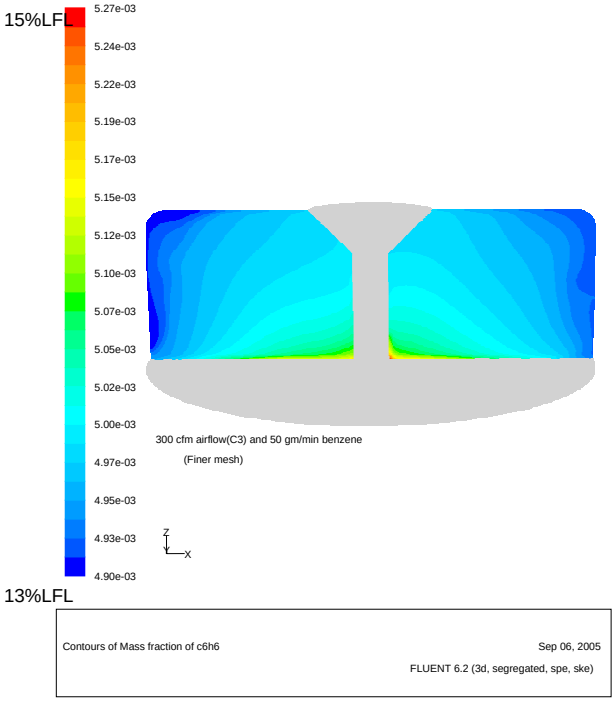

(Case-1A: 300 cfm airflow and 50 gm/min benzene generation rate with about 2 million nodes)

Figure 15. Comparison of benzene mass fractions between the two cases

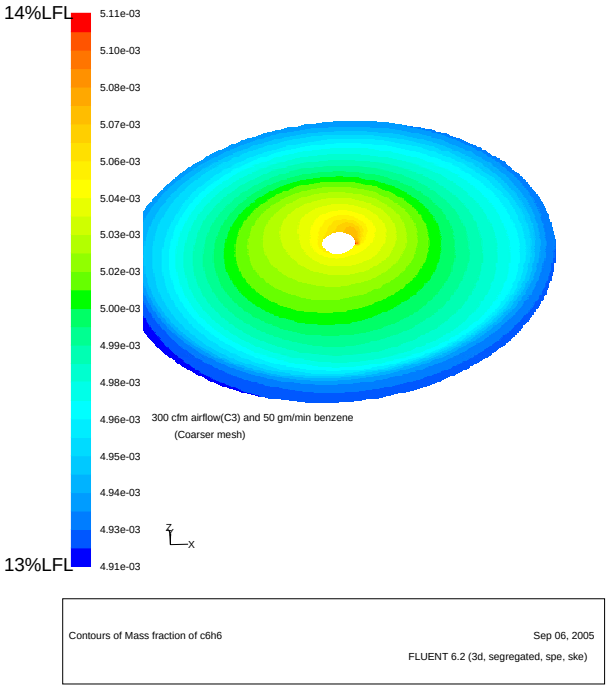

(Case-1: 300 cfm airflow and 50 gm/min benzene generation rate with about 1 million nodes)

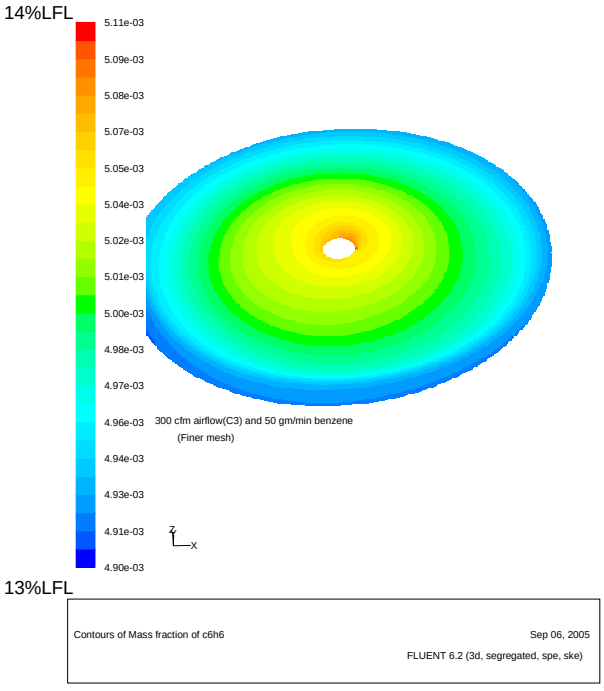

(Case-1A: 300 cfm airflow and 50 gm/min benzene generation rate with about 2 million nodes)

Figure 16. Comparison of benzene mass fractions between the two cases at 1-m elevation above the liquid surface

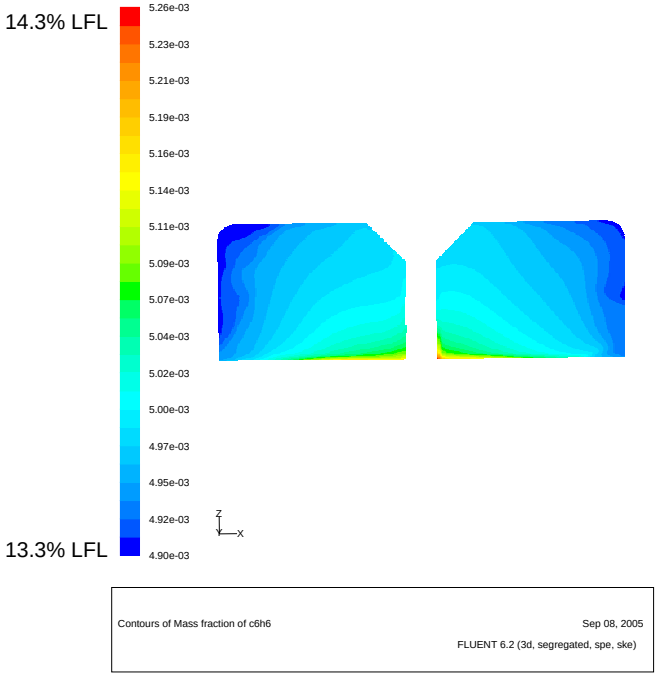

(Initial benzene concentrations established by the Case-1 conditions)

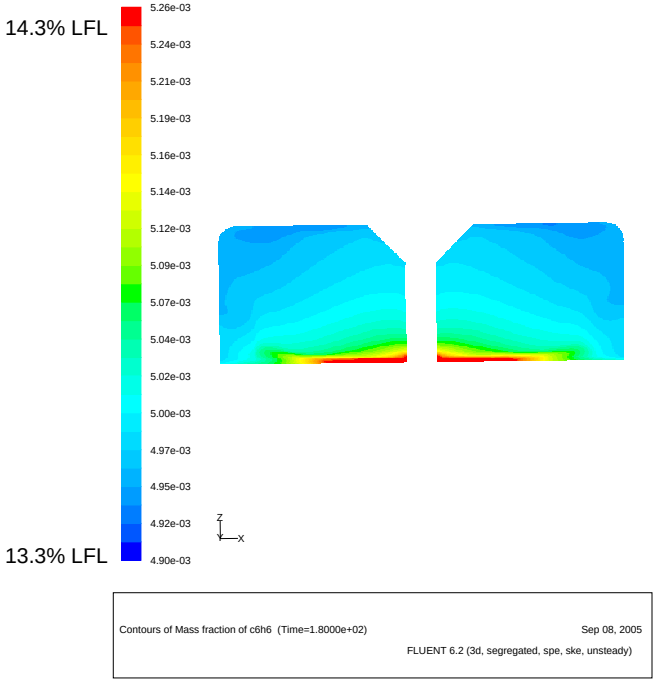

(Case-1C: Benzene concentrations at 3 min. of transient time after stopping the air purging of the Case-1 conditions)

Figure 17. Transient responses of benzene concentrations of the tank vapor space to the zero inlet airflow conditions with the Case-1 results used as the initial conditions.

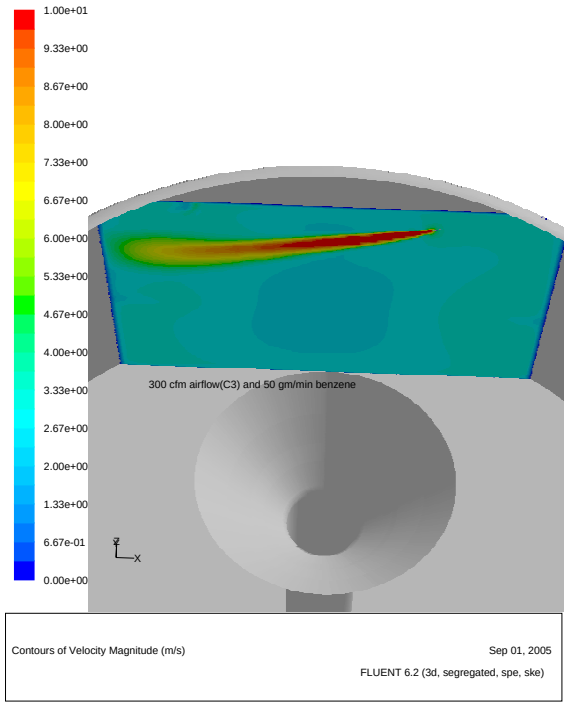

(Case-1: 300 cfm airflow and 50 gm/min benzene generation rate)

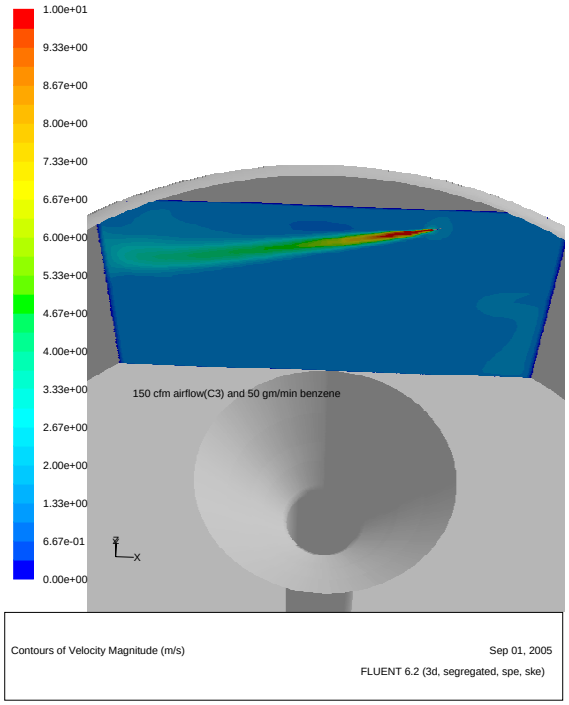

(Case-2: 150 cfm airflow and 50 gm/min benzene generation rate)

Figure 18. Comparison of gas velocity distributions at the vertical plane crossing the gas inlet nozzle between the two cases under the same color scaling system

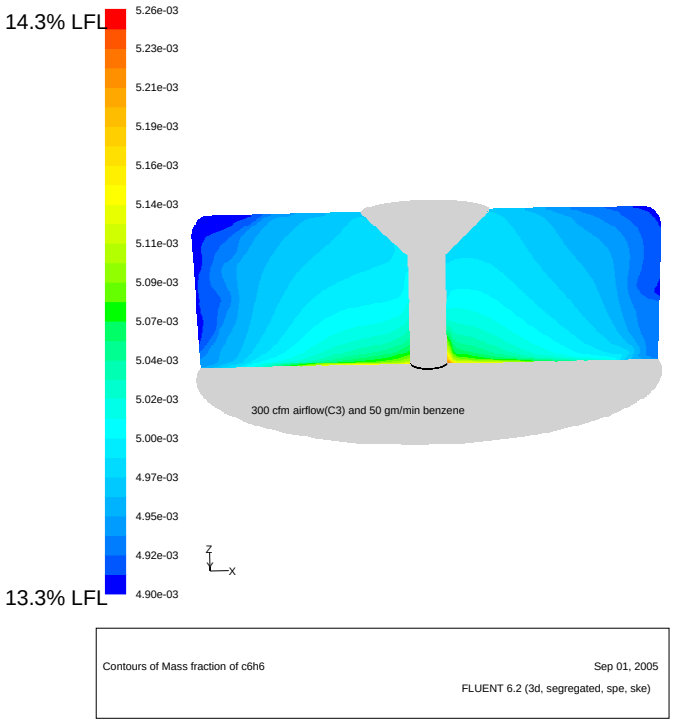

(Case-1: 300 cfm airflow and 50 gm/min benzene generation rate)

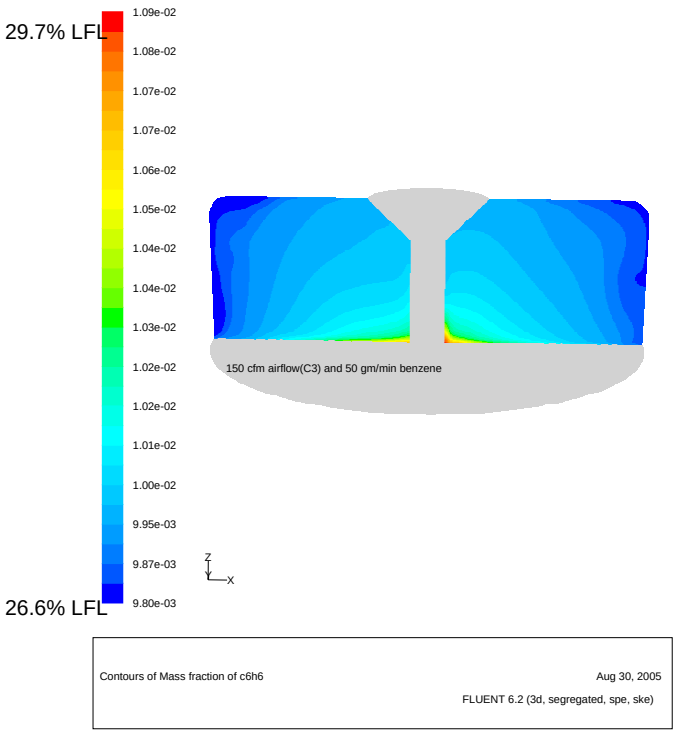

(Case-2: 150 cfm airflow and 50 gm/min benzene generation rate)

Figure 19. Comparison of benzene mass fractions between the two cases

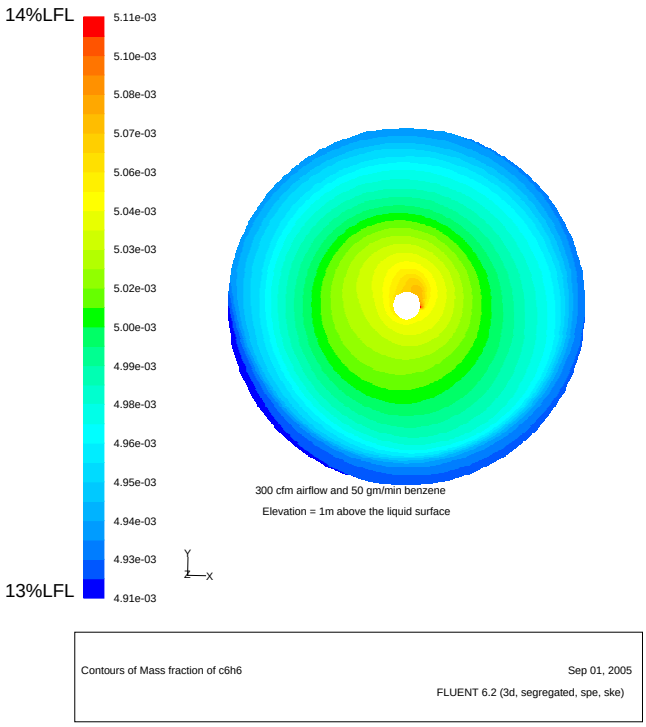

(Case-1: 300 cfm airflow and 50 gm/min benzene generation rate)

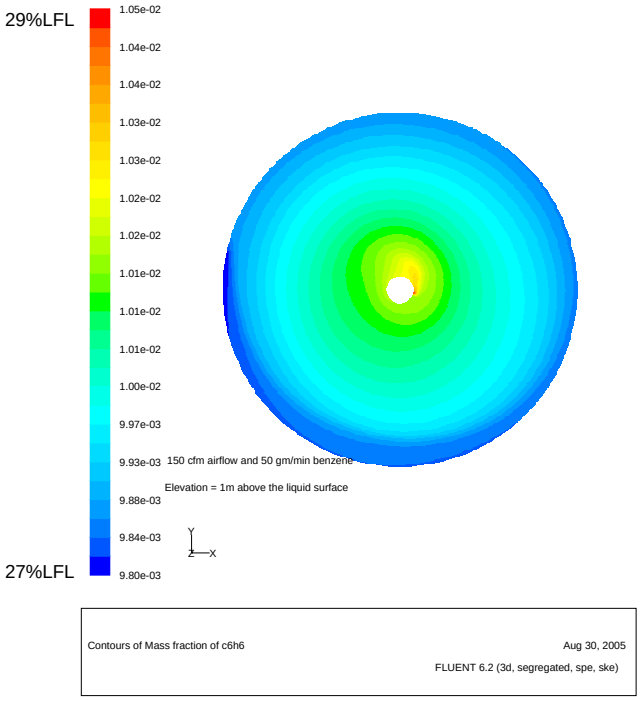

(Case-2: 150 cfm airflow and 50 gm/min benzene generation rate)

Figure 20. Comparison of benzene mass fractions between the two cases

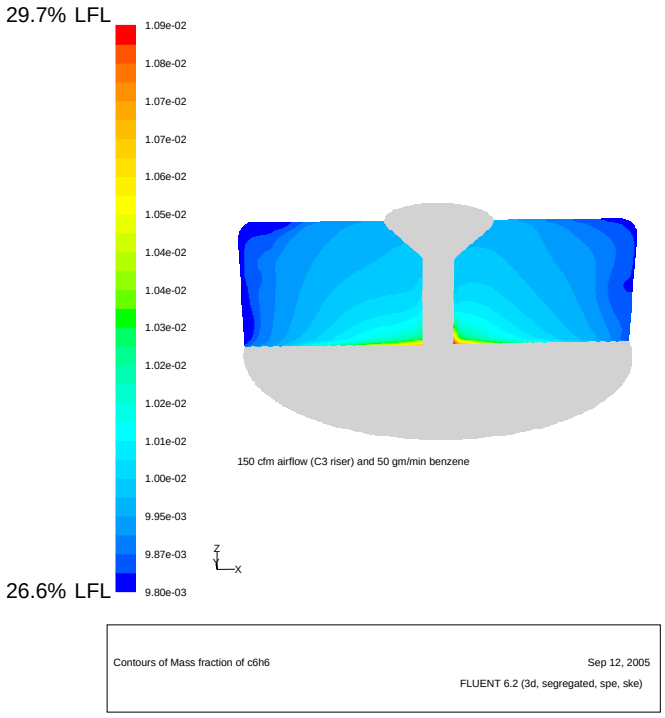

(Case-2: 150 cfm airflow through C3 riser nozzle and 50 gm/min. benzene)

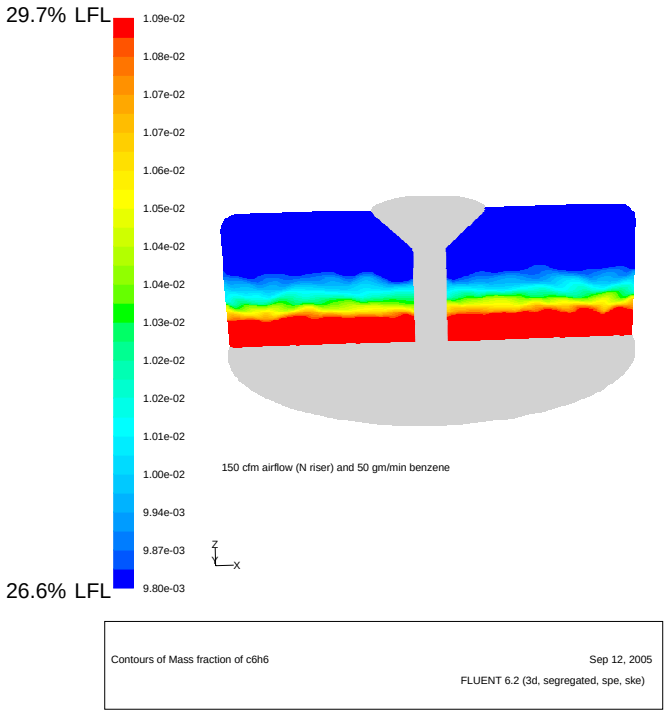

(Case-3: 150 cfm airflow through N riser nozzle and 50 gm/min. benzene)

Figure 21. Comparison of benzene mass fractions between the two cases under the same color scale

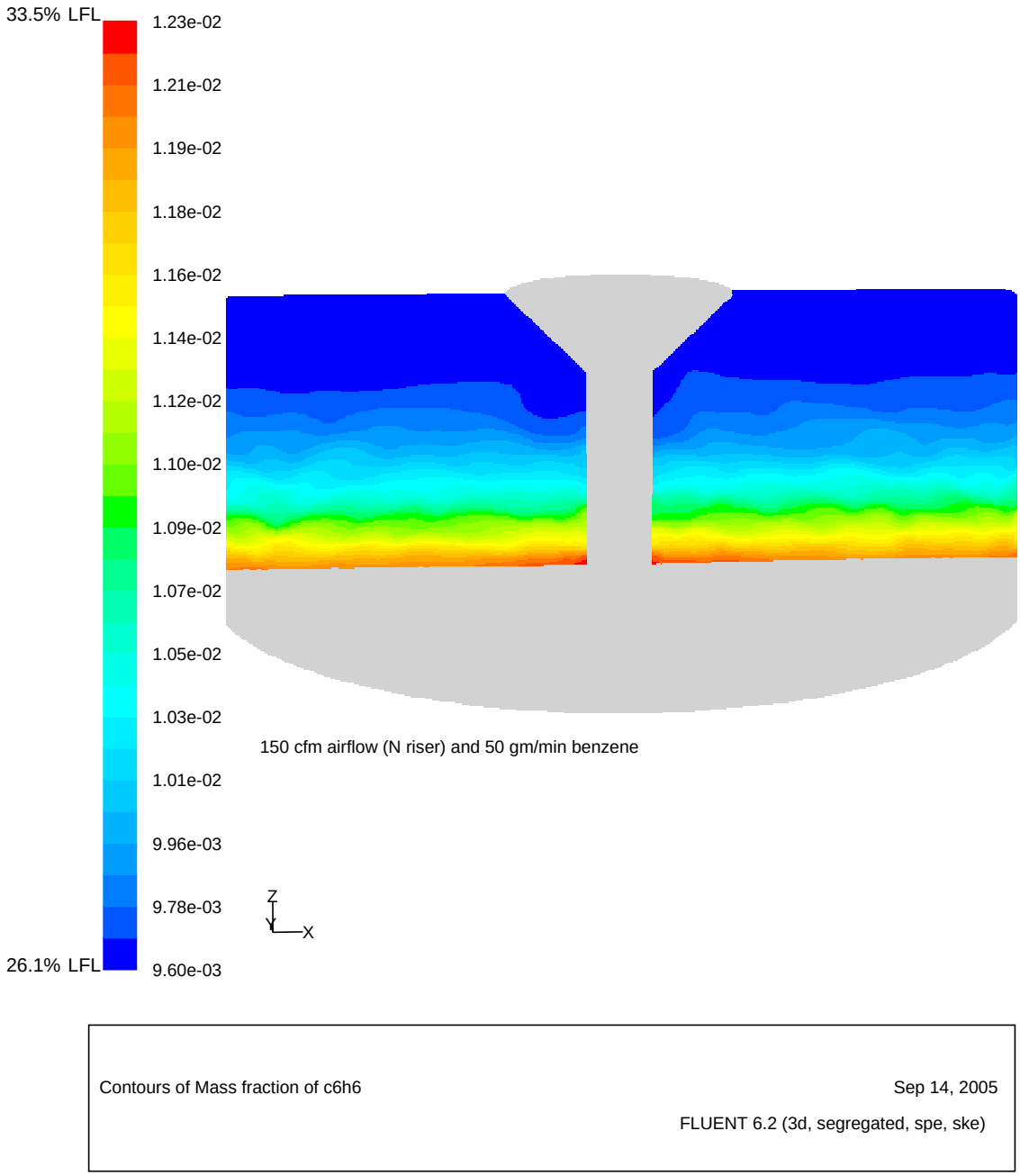

Figure 22. Benzene mass fraction distributions for Case-3 under the full-scale color code system

Table 4. Summary of the calculated results for the cases considered in the present study

Cases	Air inlet location (size)	Air flowrate at inlet (ft^3/min)	Benzene generation (gm/min)	Max. benzene concentration (vol. %)	% benzene LFL value*
Reference (Initial case)	C3 riser (1 in)	300	400	1.63	119
Case-1	C3 riser (1 in)	300	50	0.20	15
Case-1A	C3 riser (1 in)	300	50	0.20	15
Case-2	C3 riser (1 in)	150	50	0.41	30
Case-3	N riser (6 in)	150	50	0.46	34

Note:* % LFL value is based on benzene LFL of 1.37 vol.% at 25^{o}C.

4. Summary and Conclusions

A computational fluid dynamics (CFD) model was developed to estimate maximum benzene concentration for the vapor space domain inside Tank 48. The CFD model took a three-dimensional momentum-species transport coupled approach. The flow conditions for the operations are assumed to be fully turbulent since Reynolds numbers for typical operating conditions are in the range of 50,000 to 500,000 based on the inlet conditions of the air purging system. A standard two-equation turbulence model was used for this work. A series of sensitivity runs was performed to establish the numerical validity of the results.

The calculations included nominal boundary conditions for air inlet and exhaust, as well as benzene evolution from the tank liquid surface. Additional calculations included a reduced benzene evolution rate, reduced air inlet and exhaust flow, and a modified air inlet location. The calculations were based on prototypic tank geometry and nominal operating conditions.[1, 2] Detailed cases considered in the scoping calculations are provided in Table 1.

The flow patterns in the vapor space demonstrate that with ventilation air entering the tank through a 1-in nozzle near the C3 riser, the benzene gas is fairly well mixed before leaving the tank via the J riser. Mixing is not as good when air enters through the 6-inch opening in the N-riser with no nozzle to accelerate or direct the air. The modeling results showed that benzene concentrations were relatively low for all typical operating configurations and conditions. All the modeling calculations addressing sensitivity issues such as differencing options, mesh density, and transient performance

demonstrated that the scoping model could capture the necessary phenomena without introducing nonphysical behavior because of the numerical discretization. Therefore, refining and upgrading the present scoping model is recommended for support of safety class calculations.

5. References

1. "T48 Vapor Space Modeling: Status", E-mail sent by Satish Shah, August 15, 2005.

2. "T48 CFD", E-mail sent by Satish Shah, August 30, 2005.

3. J. H. Perry, *Chemical Engineer's Handbook*, McGraw-Hill Book Company, Inc., 3rd Edition, 1950.

4. *FLUENT6*, Fluent, Inc., 2005.

5. S. Y. Lee, R. A. Dimenna, D. B. Stefanko, R. A. Leishear, "Mixing in Large Scale Tanks – Part I, Flow Modeling of turbulent Mixing Jets," ASME Heat Transfer / Fluids Engineering Conference, Charlotte, N. C., July 11 – 15, 2004.

6. W. P. Jones and P. E. Launder, "The Prediction of Laminarization with a Two-Equation Model of Turbulence", Int. Journal of Heat and Mass Transfer, Vol. 15, pp. 301-314, 1972.